7.3 Nonlinear Approach to the Calculation of Oscillator Phase Noise

By Dr. Ulrich L. Rohde, N1UL

The mechanism of noise generation in an oscillator combines the equivalent of frequency conversion (mixing) with the effect of AM-to-PM conversion. Therefore, to calculate oscillator phase noise, we must first be able to calculate the noise figure of a mixer [75]. This chapter presents the use of an algorithm for the computation of SSB carrier noise in free running oscillators using the harmonic balance (HB) nonlinear technique.

Traditional approaches relying on frequency conversion analysis are not sufficient to describe the complex physical behavior of a noisy oscillator. The accuracy of this nonlinear approach is based on the dynamic range of the harmonic balance simulator and the quality of the parameter extraction for the active device. The algorithm described has also been verified with several examples up to millimeter wavelengths. This is the only algorithm that provides a complete and rigorous treatment of noise analysis for autonomous circuits without restrictions such as not being able to handle memory effects.

Noise Generation in Oscillators

As shown above, the qualitative linearized picture of noise generation in oscillators is very well known. The physical effects of random fluctuations taking place in the circuit are different depending on their spectral allocation with respect to the carrier:

- Noise components at low frequency deviations result in frequency modulation of the carrier through mean square frequency fluctuation proportional to the available noise power.
- Noise components at high frequency deviations result in phase modulation of the carrier through mean square phase fluctuation proportional to the available noise power.

We will demonstrate that the same conclusions can be quantitatively derived from the HB equations for an autonomous circuit.

Equivalent Representation of a Noisy Nonlinear Circuit

A general noisy nonlinear network can be described by the equivalent circuit shown in Figure 7-13 and Appendix D. The circuit is divided into linear and nonlinear subnetworks as noise-free mult8-ports. Noise generation is accounted for by connecting a set of noise voltage and noise current sources at the ports of the linear subnetwork [76-80].

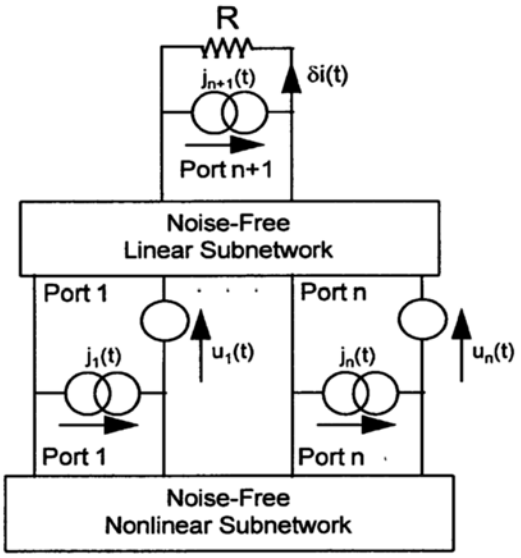

Figure 7-13 Equivalent circuit of a general noisy nonlinear network.

Frequency Conversion Approach

The circuit supports a large signal time periodic steady state of fundamental angular frequency ω_0 (carrier). Noise signals are small perturbations superimposed on the steady state, represented by families of pseudo-sinusoids located at the sidebands of the carrier harmonics. Therefore, the noise performance of the circuit is determined by the exchange of the power among the sidebands of the unperturbed steady state through frequency conversion in the nonlinear subnetwork. Due to the perturbative assumption, the nonlinear subnetwork can be replaced with a mult8-frequency linear mult8-port described by a conversion matrix. The flow of noise signals can be computed by means of conventional linear circuit techniques.

The frequency conversion approach frequently used has the following limitations:

The frequency conversion approach is not sufficient to predict the noise performance of an autonomous circuit. The spectral density of the output noise power, and consequently the PM noise computed by the conversion analysis are proportional to the available power of the noise sources.

- In the presence of both thermal and flicker noise sources, PM noise: raises as ω^{-1} for $\omega \to 0$; tends to a finite limit for $\omega \to \infty$.

- Frequency conversion analysis: correctly predicts the far carrier noise behavior of an oscillator, and in particular the oscillator noise floor; does not provide results consistent with the physical observations at low deviations from the carrier.

This inconsistency can be removed by adding the modulation noise analysis. In order to determine the far away noise using the autonomous circuit perturbation analysis, the following applies:

The circuit supports a large signal time periodic autonomous regime. The circuit is perturbed by a set of small sources located at the carrier harmonics and at the sidebands at a deviation ω from carrier harmonics. The perturbation of the circuit state $(\delta \mathbf{X}_B, \delta \mathbf{X}_H)$ is given by the uncoupled sets of equations:

$$\frac{\partial E_B}{\partial E_B} \delta X_B = J_B(\omega) \tag{7-36}$$

$$\frac{\partial E_H}{\partial E_H} \delta X_H = J_H(\omega) \tag{7-37}$$

where

E_B, E_H = vectors of HB errors
X_B, X_H = vectors of state variable (SV) harmonics (since the circuit is autonomous, one of the entries X is replaced by the fundamental frequency ω_0)
J_B, J_H = vectors of forcing terms

The subscripts B and H denote sidebands and carrier harmonics, respectively.

For a spot noise analysis at a frequency ω, the noise sources can be interpreted in either of two ways:

- Pseudo-sinusoids with random amplitude and phase located at the sidebands. Noise generation is described by Equation (7-36) which is essentially a frequency conversion equation relating the sideband harmonics of the state variables and of the noise sources. This description is exactly equivalent to the one provided by the frequency conversion approach. This mechanism is referred to as *conversion noise* [70-79].

- Sinusoids located at the carrier harmonics, randomly phase- and amplitude-modulated by pseudo-sinusoidal noise at frequency ω. Noise generation is described by Equation (7-37), which describes noise-induced jitter of the circuit-state, represented by the vector δX_H. The modulated perturbing signals are represented by replacing the entries of J_H with the complex modulation laws. This mechanism is referred to as *modulation noise*. One of the entries of δX_H is $\delta\omega_0$

where $\delta\omega_0(\omega)$ = phasor of the pseudo-sinusoidal components of the fundamental frequency fluctuations in a 1 Hz band at frequency ω. Equation (7-37) provides a frequency jitter with a mean square value proportional to the available noise power. In the presence of both thermal and flicker noise, PM noise raises as ω^{-3} for $\omega \to 0$ and tends to 0 for $\omega \to \infty$. Modulation noise analysis correctly describes the noise behavior of an oscillator at low deviations from the carrier and does not provide results consistent with physical observations at high deviations from the carrier.

The combination of both phenomenon explains the noise in the oscillator shown in Figure 7-14, where the near carrier noise dominates below ω_X and far carrier noise dominates above ω_X. Figure 7-15 (itemized form) shows the noise sources as they are applied at the IF. We have arbitrarily defined the low oscillator output as IF. This applies to the conversion matrix calculation.

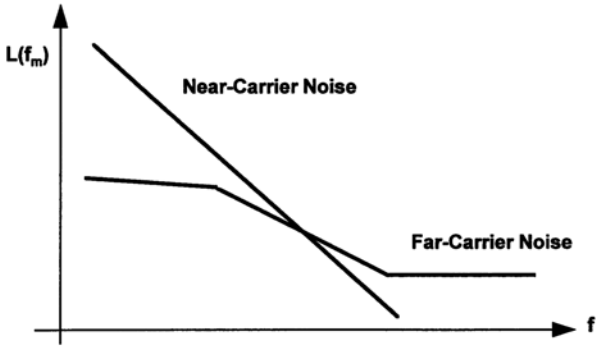

Figure 7-14 Oscillator noise components.

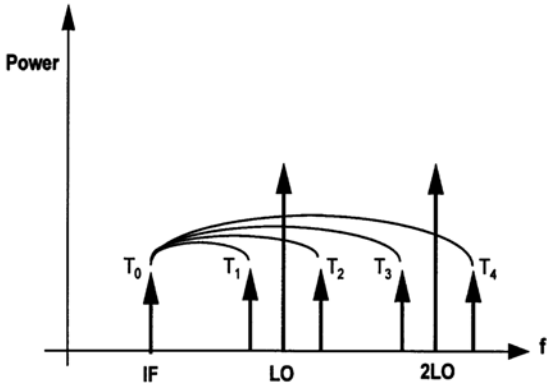

Figure 7-15 Noise sources where the noise at each sideband contributes to the output noise at the IF through frequency conversion.

Figure 7-16 shows the total contribution which have to be taken into consideration for calculation of the noise at the output. The accuracy of the calculation of the phase noise depends highly on the quality of the parameter extraction for the nonlinear device; in particular, high frequency phenomena must be properly modeled. In addition, the flicker noise contribution is essential. This is also valid for mixer noise analysis.

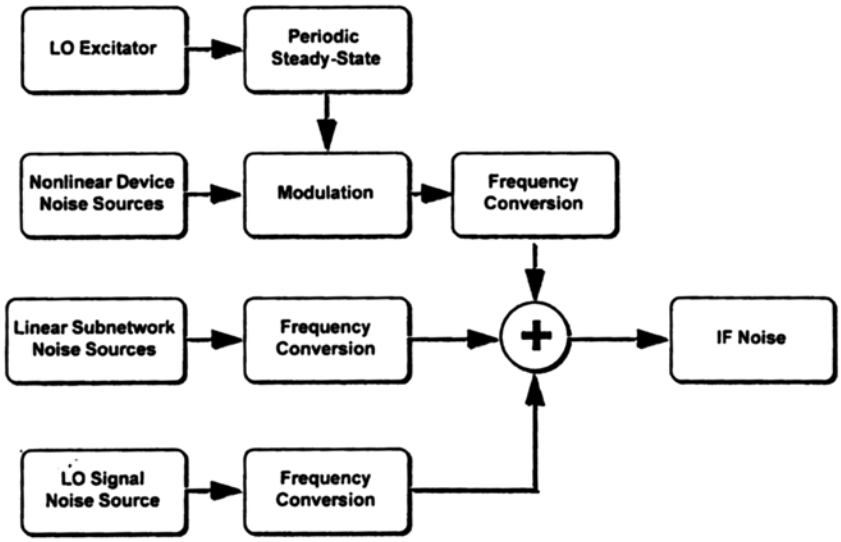

Figure 7-16 Noise mechanisms.

Conversion Noise Analysis

The actual mathematics used to calculate the noise result (Ansoft Serenade 8.*x*) are as follows:

*k*th harmonic PM noise:

$$\left\langle \left|\delta\Phi_k(\omega)\right|^2 \right\rangle = \frac{N_k(\omega) - N_{-k}(\omega) - 2\,\mathrm{Re}\left[C_k(\omega)\right]}{R\left|I_k^{SS}\right|^2} \tag{7-38}$$

*k*th harmonic AM noise:

$$\left\langle \left|\delta A_k(\omega)\right|^2 \right\rangle = 2\,\frac{N_k(\omega) - N_{-k}(\omega) + 2\,\mathrm{Re}\left[C_k(\omega)\right]}{R\left|I_k^{SS}\right|^2} \tag{7-39}$$

*k*th harmonic PM-AM correlation coefficient:

$$C_k^{PMAM}(\omega) = \left\langle \delta\Phi_k(\omega)\delta A_k(\omega)^* \right\rangle = -\sqrt{2}\,\frac{2\,\mathrm{Im}[C_k(\omega)] + j[N_k(\omega) - N_{-k}(\omega)]}{R\left|I_k^{SS}\right|^2} \tag{7-40}$$

where

$N_k(\omega)$, $N_{-k}(\omega)$ = noise power spectral densities at the upper and lower sidebands of the *k*th harmonic
$C_k(\omega)$ = normalized correlation coefficient of the upper and lower sidebands of the *k*th carrier harmonic
R = load resistance
I_k^{ss} = *k*th harmonic of the steady-state current through the load.

Modulation Noise Analysis

*k*th harmonic PM noise:

$$\left\langle \left|\delta\Phi_k(\omega)\right|^2 \right\rangle = \frac{k^2}{\omega^2}\mathbf{T}_F \left\langle \mathbf{J}_H(\omega)\mathbf{J}_H^t(\omega) \right\rangle \mathbf{T}_F^t \tag{7-41}$$

*k*th harmonic AM noise:

$$\left\langle \left|\delta A_k(\omega)\right|^2 \right\rangle = \frac{2}{\left|I_k^{SS}\right|^2}\mathbf{T}_{Ak} \left\langle \mathbf{J}_H(\omega)\mathbf{J}_H^t(\omega) \right\rangle \mathbf{T}_{Ak}^t \tag{7-42}$$

*k*th harmonic PM-AM correlation coefficient:

$$C_k^{PMAM}(\omega) = \left\langle \delta\Phi_k(\omega)\delta A_k(\omega)^* \right\rangle = \frac{k\sqrt{2}}{j\omega\left|I_k^{SS}\right|^2}\mathbf{T}_F \left\langle \mathbf{J}_H(\omega)\mathbf{J}_H^t(\omega) \right\rangle \mathbf{T}_{Ak}^t \tag{7-43}$$

where

$J_H(\omega)$ = vector of Norton equivalent of the noise sources
T_F = frequency transfer matrix
R = load resistance
I_k^{ss} = *k*th harmonic of the steady-state current through the load

Experimental Variations

We will look at two examples where we compare predicted and measured data. Figure 7-17 shows the abbreviated circuit of a 10 MHz crystal oscillator. It uses a high

precision, high Q crystal made by companies such as Bliley. Oscillators like this are intended for use as frequency and low phase noise standards. In this case, the circuit under consideration is part of the HP3048 phase noise measurement system.

Figure 7-18 shows the measured phase noise of this HP frequency standard, and Figure 7-19 shows the phase noise predicted using the mathematical approach outlined above.

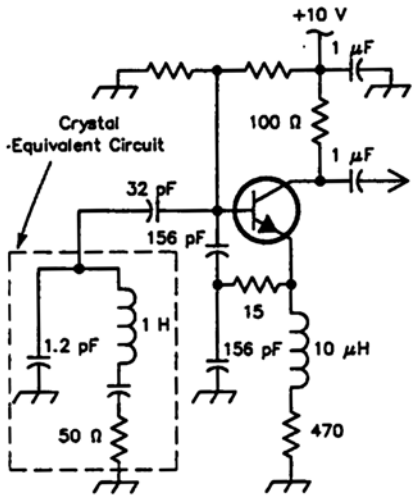

Figure 7-17 Abbreviated circuit of a 10-MHz crystal oscillator.

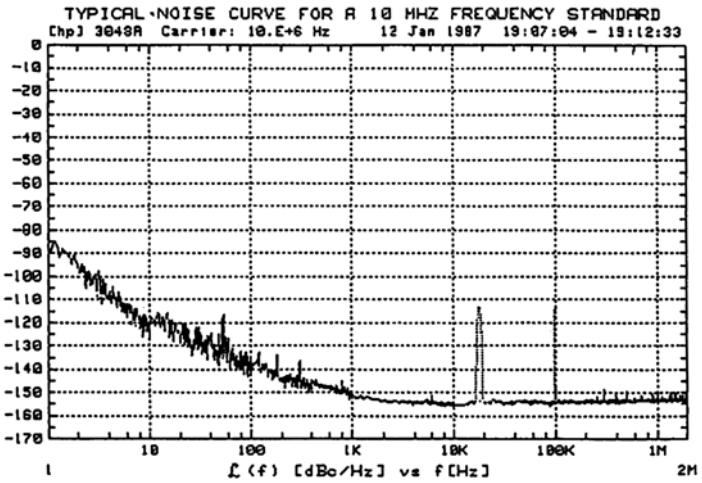

Figure 7-18 Measured phase noise for this frequency standard by HP.

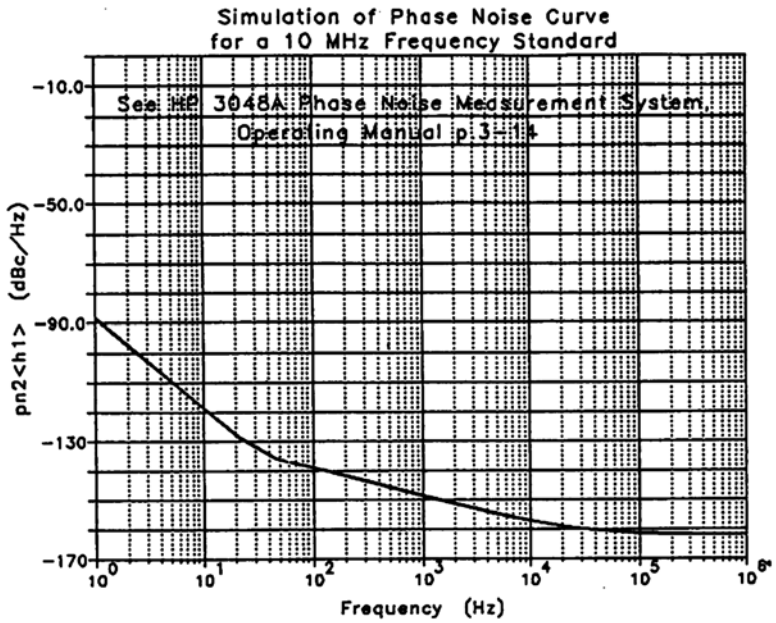

Figure 7-19 Simulated phase noise of the oscillator shown in Figure 7-17.

In co-operation with Motorola, an 800 MHz VCO was analyzed. The parameter extraction for the Motorola transistor was done. Figure 7-20 shows the circuit, which is a Colpitts oscillator that uses RF feedback in the form of a 15 Ω resistor between the emitter and the capacitive voltage divider. The tuned circuit is loosely coupled to this part of the transistor circuit. Figure 7-21 shows a plot of the measured and predicted phase of this circuit..

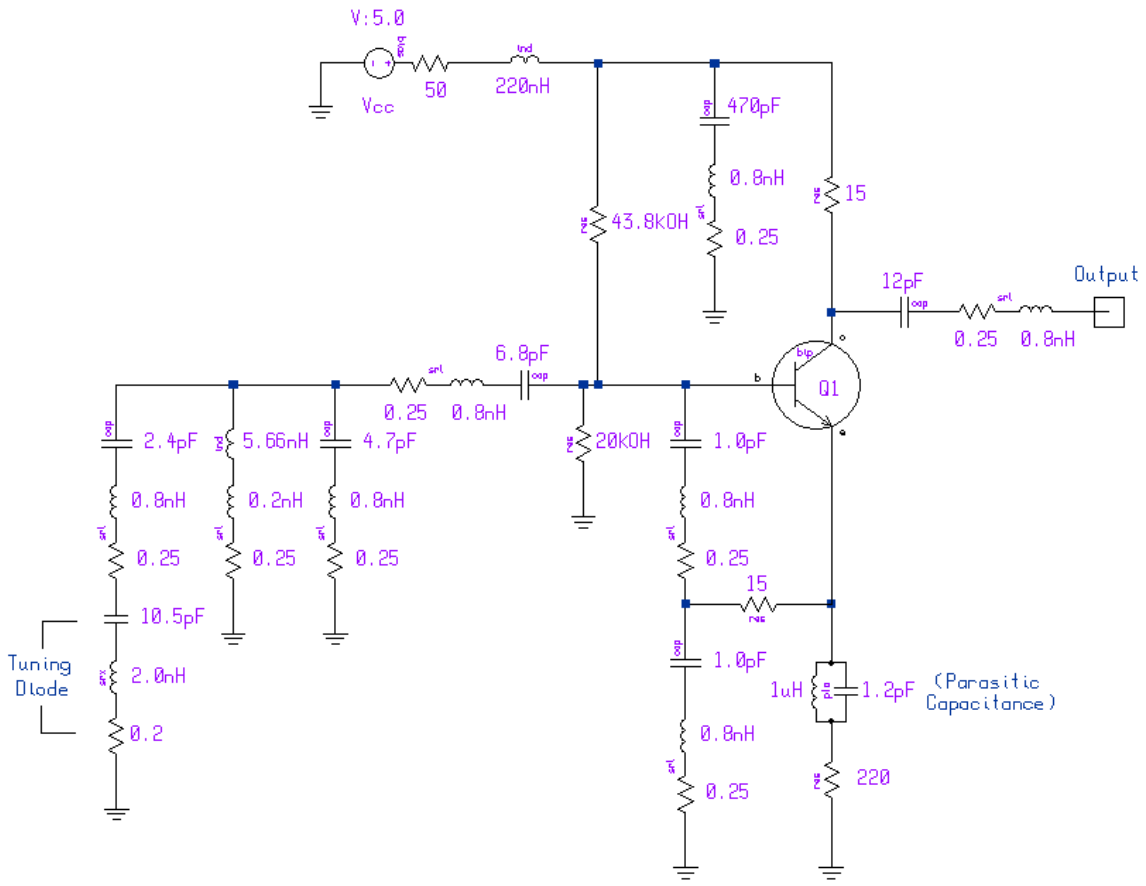

Figure 7-20 Colpitts oscillator that uses RF negative feedback between the emitter and capacitive voltage divider. To be realistic, we have also used real components rather than ideal ones. The suppliers for the capacitors and inductors provide some typical values for the parasitics. The major changes are 0.8 nH and 0.25 Ω in series with the capacitors. The same thing applies for the main inductance, which has a parasitic connection inductance of 0.2 nH in series with a 0.25 Ω resistance. These types of parasitics are valid for a fairly large range of components assembled in surface mount applications. Most engineers model the circuit only by assuming lossy devices, not adding these important parasitics. One of the side effects we have noticed is that the output power is more realistic and, needless to say, the simulated phase noise agrees quite well with measured data. This circuit can also serve as an example for modeling amplifiers and mixers using surface mount components.

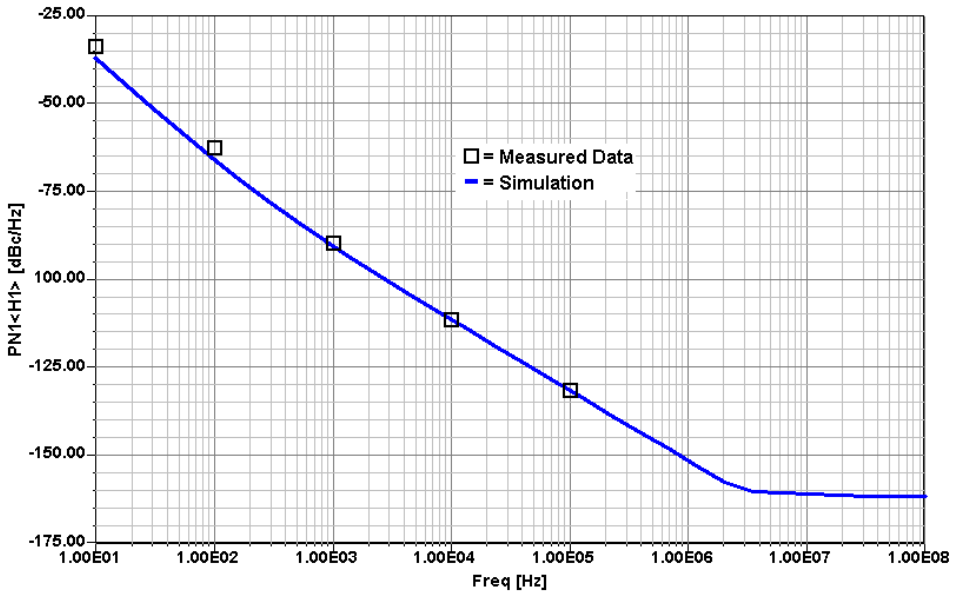

Figure 7-21 Comparison between predicted and measured phase noise for the oscillator shown in Figure 7-20.

The harmonic balance simulator Microwave Harmonica/Designer, which has been used for many cross-checks, is based on the principle shown above and shows extremely high accuracy in noise predictions. The harmonic balance simulator cannot be substituted by a set of equations because the harmonic balance process works iteratively, therefore, such a simulator is necessary in parallel to all the equations which are being derived to be used as a validation tool. An extreme example of its usefulness was the case where one of the previously shown oscillators was optimized for best output power with an assumed Q of 200 of the resonator circuit itself. In a following simulation, the value of Q was increased from 200 to 400 to examine the results. The output power remained the same, but the phase noise deteriorated. This contradicts practical experience for optimized oscillators. The surprising result can be explained by the fact that a particular parallel resonant value was assumed, and the values of C_1 and C_2 were calculated. By increasing the Q, the feedback ratio generated too much gain, more than necessary, and therefore, the phase noise became worse. This is an experiment which is normally not done when building oscillators, but shows the power of the CAD tool and the insight it provides into the inner workings of the oscillator.